² Morth, R. and Speyer, J. L., "Divergence from equilibrium glide path at supersatellite velocities," ARS J. 31, 448-450 (1961)

³ Norman, W. S. and Meier, T. C., "Approximate longitudinal dynamics of a lifting orbital vehicle," U. S. Air Force Academy, USAFA TN 63-1 (January 15, 1963).

Optimum Deboost Altitude for Specified Atmospheric Entry Angle

JEROME M. BAKER*

The Marquardt Corporation, Van Nuys, Calif.

Bruce E. Baxter†

Lockheed Aircraft Corporation, Burbank, Calif.

AND

Paul D. Arthur‡

University of Southern California, Los Angeles, Calif.

Nomenclature

h = altitude

r = radius

V = velocity

 $\Delta V = \text{velocity increment}$

 β = retrofire orientation angle

 γ = elevation angle above local horizontal

Subscripts

0 = conditions at planet radius

1 = conditions at initial altitude

c = circular

E = conditions at entry altitude

Introduction

TECHNIQUES for the controlled recovery of a re-entry vehicle by impulsive deboost are well known. The general problem has been discussed by Low¹ for near-earth orbits through a linearization technique. Detra, Riddell, and Rose² have examined the problem with respect to some of the limitations imposed by weight and accuracy requirements. Galman³ and Low¹ have discussed maximizing the atmospheric entry angle for a given retrorocket velocity decrement.

The purpose of this note is to show that there is a minimum (retrofire) impulse with respect to altitude for a given entry angle. This result suggests that a mission altitude could be selected for minimum deboost requirement. It is also shown that minimizing the retrofire impulse with respect to retrofire angle is equivalent to maximizing the atmospheric entry angle (the problem investigated by Low¹ and by Galman³).

Analysis

Consider a vehicle initially in a circular orbit as shown in Fig. 1. From the conservation of energy and angular momentum,

$$V_{1}^{2} - 2V_{c_{1}}^{2} = V_{E}^{2} - 2V_{c_{1}}^{2}(r_{1}/r_{E})$$
 (1)

$$r_1 V_1 \cos \gamma_1 = r_E V_E \cos \gamma_E \tag{2}$$

Also, from geometric considerations,

$$V_{1}^{2} = V_{c_{1}}^{2} + (\Delta V)^{2} - 2V_{c_{1}}\Delta V \cos\beta \tag{3}$$

Received February 11, 1963.

$$V_1 \cos \gamma_1 = V_{c_1} - \Delta V \cos \beta \tag{4a}$$

or the equivalent

$$V_1/\sin\beta = \Delta V/\sin\gamma_1 \tag{4b}$$

It should be noted that the entry angle γ_E is a function of both the retrorocket alignment angle β and the impulsive velocity decrement ΔV . Therefore, for constant γ_E ,

$$\left. \frac{\partial \Delta V}{\partial \beta} \right|_{\gamma_E} = -\left. \frac{\partial \gamma_E}{\partial \beta} \right|_{\Delta V} \div \left. \frac{\partial \gamma_E}{\partial \Delta V} \right|_{\beta} \tag{5}$$

If the alignment angle β is found which maximizes γ_E ($\partial \gamma_E / \partial \beta|_{\Delta V} = 0$), then the minimum ΔV for a given entry angle also has been found $(\partial \Delta V / \partial \beta|_{\gamma_E} = 0)$ provided that $\partial \gamma_E / \partial \Delta V|_{\mathcal{S}} \neq 0$

As shown by Galman, $\partial \gamma_E / \partial \beta |_{\Delta V}$ is given by

$$\frac{\partial \gamma_E}{\partial \beta} \bigg|_{\Delta V} = \frac{\Delta V \sin \beta}{V_E^2 (V_{c_1} - \Delta V \cos \beta)} \times \left[V_{c_1} \Delta V \cos \beta - (\Delta V)^2 + 2V_{c_1}^2 \left(1 - \frac{r_1}{r_E} \right) \right] \frac{1}{\tan \gamma_E}$$
(6)

with the zero roots at

$$\sin\beta = 0 \tag{7a}$$

$$\cos\beta = \Delta V/V_{c_1} + \frac{2[(r_1/r_B) - 1]}{\Delta V/V_{c_1}}$$
 (7b)

By using Eqs. (1-4), $\partial \gamma_E / \partial \Delta V|_{\beta}$ is given by

$$\left. \frac{\partial \gamma_E}{\partial \Delta V} \right|_{\beta} = \underbrace{\left\{ \frac{V_{c_1} \Delta V \sin^2 \beta - 2 V_{c_1}^2 [1 - (r_1/r_B)] \cos \beta}{V_E^2 (V_{c_1} - \Delta V \cos \beta)} \right\}}_{\text{tan} \gamma_B} \tag{8}$$

But this expression can be zero only when

$$\cos\beta = \frac{(r_1/r_E) - 1}{\Delta V/V_{c_1}} \pm \left\{ 1 + \left[\frac{(r_1/r_E) - 1}{\Delta V/V_{c_1}} \right]^2 \right\}^{1/2} \quad (9)$$

It is evident that Eqs. (7b) and (9) never can be equal for nonzero values of ΔV . Therefore, the β given by Eq. (7) will yield the maximum value of γ_E and the minimum value of ΔV for a fixed orbital altitude. For $\beta = 0$, the minimum value of ΔV is obtained by using Eqs. (1-4) and (7a) to eliminate V_E , V_1 , γ_1 , and β :

$$\frac{\Delta V}{V_{c_E}}\Big|_{\beta=0} = \left(\frac{r_E}{r_1}\right)^{1/2} \times \left\{1 - \frac{r_E}{r_1} \cos\gamma_E \left[\frac{2[(r_1/r_E) - 1]}{1 - [(r_E/r_1)\cos\gamma_E]^2}\right]^{1/2}\right\} (10)$$

For $\beta \neq 0$, the minimum ΔV is given by

$$\frac{\Delta V}{V_{c_E}}\Big|_{\min} = \left\{ \frac{r_E}{r_1} \left[1 - \left(\frac{r_E}{r_1} \cos \gamma_E \right)^2 - 2 \left(\frac{r_1}{r_E} - 1 \right) \right] \right\}^{1/2}$$
(11)

The optimum retrorocket alignment angle is found by combining Eqs. (7b) and (11):

$$\cos\beta)_{\text{opt}} = \frac{1 - (r_E/r_1 \cos\gamma_E)^2}{\{1 - (r_E/r_1 \cos\gamma_E)^2 - 2[(r_1/r_E) - 1]\}^{1/2}}$$
(12)

The velocity decrements and the alignment angle given by Eqs. (10–12) are shown in Fig. 2§ for various values of atmospheric entry angle and radius ratio r_1/r_0 . For a given γ_B and for small radius ratios, Fig. 2 shows that it is advantageous to operate at the optimum alignment angle given by Eq. (12). As the radius ratio increases, the alignment angle decreases

^{*} Senior Research Engineer, ASTRO; presently Member of the Technical Staff, Aerospace Corporation. Member AIAA.

[†] Senior Thermodynamics Engineer, Spacecraft Organization. ‡ Adjunct Professor, Aerospace Engineering. Associate Fellow Member AIAA.

 $[\]$ Appreciation is expressed to Linda Gardner of Marquardt for programming the equations.

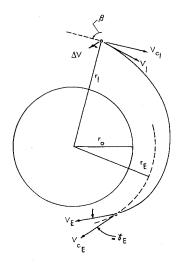


Fig. 1 Transfer orbit geometry (note: radii not to scale, γ_E defined at 400,000 ft)

rapidly to zero, at which point the minimum ΔV is given by Eq. (10). The $\beta = 0$ boundary is obtained by setting $\cos \beta = 1$ in Eq. (7b):

$$\frac{\Delta V}{V_{c_E}} = \left(\frac{r_E}{r_1}\right)^{1/2} \left[\frac{1}{2} \pm \frac{1}{2} \left(9 - 8\frac{r_1}{r_E}\right)^{1/2}\right] \tag{13}$$

Figure 2 shows a relative maximum ΔV occurring at a radius ratio of 5.88 for $\gamma_E = 0^{\circ}$ (in agreement with the results of Esses⁴). However, this relative maximum vanishes for increasing γ_E .

Current manned and unmanned re-entry vehicles are restricted to small entry angles due to deceleration and heating limitations. It can be seen in Fig. 2 that for small entry angles there is a well-defined minimum ΔV with respect to altitude. To show this analytically, the small-angle ap-

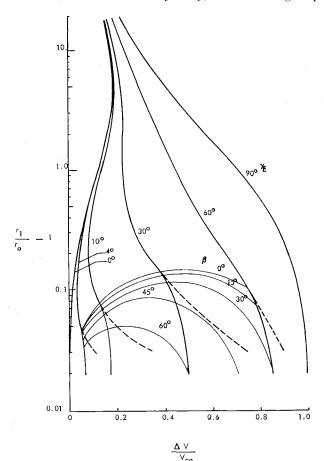


Fig. 2 Nondimensional retrofire impulse for deboost from circular orbit

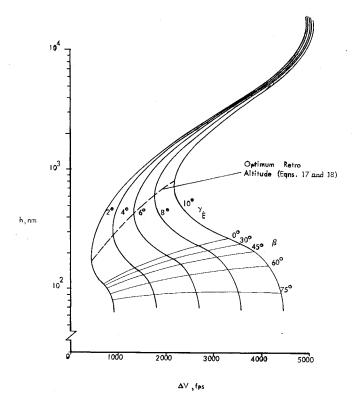


Fig. 3 Optimum retrofire altitude and retrofire angle for minimum ΔV

proximation is made:

$$\cos \gamma_E = 1 - (\gamma_E^2/2) + \dots \tag{14}$$

Use of this approximation in Eq. (10) yields (for $\beta = 0$)

$$\gamma_E = \left[1 - \frac{(r_1/r_E)^2[(\Delta V/V_{c_1}) - 1]^2}{2[(r_1/r_E) - 1] + [(\Delta V/V_{c_1}) - 1]^2}\right]^{1/2}$$
(15)

For low altitudes where $r_1/r_B-1\ll 1$, and recognizing that $\Delta V/V_{c_1}\ll 1$, Eq. (15) further simplifies to

$$\gamma_E = \left[4 \frac{\Delta V}{V_{c_1}} \left(\frac{r_1}{r_E} - 1 \right) - \left(\frac{r_1}{r_E} - 1 \right)^2 \right]^{1/2} \tag{16}$$

which is equivalent to Low's Eq. (33).

For fixed entry angle γ_B , the retrorocket velocity decrement is a minimum with respect to altitude when

$$r_1/r_E = 1 + \gamma_E \tag{17}$$

At this altitude, the required ΔV is given by

$$(\Delta V/V_{c_1})_{\min} = \gamma_E/2 \tag{18}$$

The range from deboost to entry is 90° of arc. These results are shown in Fig. 3, which is an enlarged dimensional plot of the small entry angle portion of Fig. 2. It is seen that the approximate results are in good agreement with the exact results. The approximate values are also numerically consistent with the plotted results of Ref. 2.

The $\beta = 0$ boundary [Eq. (13)] reduces to

$$\frac{\Delta V}{V_{\rm co}} = 2\left(\frac{r_1}{r_E} - 1\right) \tag{19}$$

for low altitudes. Use of Eq. (16) yields

$$\gamma_E = 7^{1/2}[(r_1/r_E) - 1] \tag{20}$$

as given by Low, 1 Eq. (52).

The low-altitude small entry angle approximation can be made when $\beta \neq 0$. Equations (11) and (12) thus linearize to

$$\Delta V/V_{c_1})_{\min} = \sin \gamma_E \tag{21}$$

$$\cos\beta = \frac{2[(r_1/r_E) - 1] + \gamma_E^2}{\{\gamma_E^2 - 3[(r_1/r_E) - 1]^2\}^{1/2}}$$
(22)

For general entry angle γ_E and $r_1 \rightarrow r_E$, Eq. (12) reduces to

$$\cos\beta = \sin\gamma_E \tag{23}$$

Equation (23) is in agreement with (22); a different result was given in Ref. 1, where $\beta \to 90^{\circ}$ as $r_1 \to r_E$.

Figure 3 shows the definite advantage of deboosting from the optimum orbital altitude. Operation at any other altitude results in increases in deboost propellant with attendant decreases in payload. The retrofire alignment angle is zero degrees at all altitudes greater than or equal to the optimum. For altitudes less than optimum, β increases from zero degrees up to the value given by Eq. (23).

References

¹ Low, G. M., "Nearly circular transfer trajectories for descending satellites," NASA TR R-3 (1959).

² Detra, R. W., Riddell, F. R., and Rose, P. H., "Controlled recovery of nonlifting satellites," ARS J. 30, 892–898 (1960).

³ Galman, B. A., "Retrorocket alignment for maximum entry angle," ARS J. 32, 977–978 (1962).

⁴ Esses, H., "Maximum ejection velocity for return from satel-

lite orbits," ARS J. 29, 592 (1959).

Method of Analyzing Laminar Air **Arc-Tunnel Heat Transfer Data**

R. J. Wethern*

Lockheed Missiles and Space Company, Palo Alto, Calif.

The Fay-Riddell equations with a non-Newtonian velocity gradient are proposed as models for evaluating laminar arc-tunnel heat transfer data. Means are suggested for ways to estimate the necessary parameters. Calculations indicate that flow can remain partially frozen even to pressures of 10 psia. Calorimeter poisoning may produce marked variations in reported effective heats of ablation.

Nomenclature

= diameter of calorimeter, ft

enthalpy, Btu/lbm

 H^* effective heat of ablation, Btu/lbm

Lewis number, $\rho D_{12}\bar{c}_p/k$ Le

ablation rate, lb/ft2-sec \dot{m}

PrPrandtl number, $\bar{c}_{p\mu}/k$

heat flux, Btu/ft²-sec

temperature, °R freestream velocity, fps V

density, lbm/ft3

viscosity, lbm/ft-sec

Subscripts

= edge of boundary layer

wall

D= dissociation

Introduction

UCH ablation test work is carried out in subsonic air arc-tunnel facilities under conditions attempting to simulate those that exist behind a re-entry shock wave. The usual objective of such tests is to obtain an effective heat of ablation for the purposes of re-entry heat shield design. This

Received February 18, 1963.

effective heat of ablation is based on the rate at which a material ablates when subjected to a certain heat flux:

$$H^* = q/\dot{m} \tag{1}$$

The effective heat of ablation is thus as dependent on the heat flux measurement as on the rate of ablation.

In an air arc tunnel, this flux often is measured by immersing a flat-faced, water-cooled calorimeter into the dissociated air stream. If the air is in thermodynamic equilibrium, the calorimeter will measure essentially the maximum heat that can be transferred to a cold body under the particular conditions of the test. If the air is not in thermodynamic equilibrium, the measured heat flux will be something less than this maximum, depending on both the degree of departure from equilibrium and the catalytic activity of the calorimeter

A measure of this departure can be obtained by subjecting the data to various theoretical models. Using the modified Fay-Riddell equation^{1, 2} as a basis for these models, one has for model 1 (equilibrium boundary layer)

$$q = \frac{0.793}{Pr_w^{0.6}} \left(\rho_e \mu_e \right)^{0.44} \left(\rho_w \mu_w \right)^{0.06} \left(h_e - h_w \right) \times \left[1 + \left(Le^{0.52} - 1 \right) \frac{h_D}{h_e} \right] \left(\frac{\pi V}{2D} \right)^{1/2}$$
(2)

for model 2 (frozen flow and a fully catalytic wall) an identical equation but with the Lewis number raised to the 0.63 power, and for model 3 (frozen flow and a noncatalytic wall) an equation identical to model 2 but where the wall enthalpy includes the dissociation enthalpy. In all three models, the last term, the velocity gradient, is that corresponding to a flat face in incompressible flow as given by Truitt.3

Experimental Data and Derived Parameters

Having these three equations, a knowledge of the calorimeter wall temperature, freestream enthalpy, pressure, and velocity allows calculating the other data necessary to check measured heat fluxes against those predicted by the three The temperature, density, viscosity, and Lewis models. number can be estimated from the work of Hansen.⁴ The degree of dissociation can be estimated from that of Gilmore.5 The dissociation enthalpy then can be calculated from the heats of dissociation of nitrogen and oxygen at 14,400 Btu/lbm and 6600 Btu/lbm, respectively. Resulting properties corresponding to the outer edge of the boundary layer are given in Table 1.

Properties at the wall are calculated for a temperature of 660°R and a pressure equal to that at the outer edge of the boundary layer. Viscosity is taken as 1.3×10^{-5} lbm/ft-sec and the Prandtl number as 0.73. For model 3, the dissociation enthalpy is added to the 200-Btu/lbm-wall enthalpy of that used in the first two cases.

Heat fluxes are calculated from Table 1, and those actually measured are given in Table 2. The difference between models 1 and 2 is so slight that in Fig. 1 only points for models 1 and 3 are plotted.

Results

The most striking result is the superior correlation obtained with the assumption of frozen flow and a noncatalytic wall. Whereas the assumptions of 1) an equilibrium boundary layer or 2) frozen flow with a fully catalytic wall lead to large scatter and consistently high results, the assumption of frozen flow and a noncatalytic wall is essentially exact at lower densities and degree of dissociation and remains preferable at higher densities. At higher densities, recombination does occur but not to the extent often assumed.

The fact that the copper calorimeter acted noncatalytically is surprising, since metals and metal oxides often are considered to be quite catalytic. If, however, a copper calorimeter

Associate Research Scientist, Materials Sciences Laboratory, Research Laboratories.